brief review

Pleural pressure distribution and its relationship to lung volume and interstitial pressure

STEPHEN J. LAI-FOOK AND JOSEPH R. RODARTE
Biomedical Engineering Center, University of Kentucky, Lexington, Kentucky 40506; and Department of Medicine, Baylor College of Medicine and Methodist Hospital, Houston, Texas 77030

LAI-FOOK, STEPHEN J., AND JOSEPH R. RODARTE. *Pleural pressure distribution and its relationship to lung volume and interstitial pressure.* J. Appl. Physiol. 70(3): 967–978, 1991.—The mechanics of the pleural space has long been controversial. We summarize recent research pertaining to pleural mechanics within the following conceptual framework, which is still not universally accepted. Pleural pressure, the force acting to inflate the lung within the thorax, is generated by the opposing elastic recoils of the lung and chest wall and the forces generated by respiratory muscles. The spatial variation of pleural pressure is a result of complex force interactions among the lung and other structures that make up the thorax. Gravity contributes one of the forces that act on these structures, and regional lung expansion and pleural pressure distribution change with changes in body orientation. Forces are transmitted directly between the chest wall and the lung through a very thin but continuous pleural liquid space. The pressure in pleural liquid equals the pressure acting to expand the lung. Pleural liquid is not in hydrostatic equilibrium, and viscous flow of pleural liquid is driven by the combined effect of the gravitational force acting on the liquid and the pressure distribution imposed by the surrounding structures. The dynamics of pleural liquid are considered an integral part of a continual microvascular filtration into the pleural space. Similar concepts apply to the pulmonary interstitium. Regional differences in lung volume expansion also result in regional differences in interstitial pressure within the lung parenchyma and thus affect regional lung fluid filtration.

ventilation distribution; pleural liquid exchange; lung fluid balance; pulmonary edema

PLEURAL PRESSURE and its measurement have been subjects of considerable controversy for many years. It has long been recognized that a nonuniform pleural surface pressure distribution is related to nonuniform lung expansion and regional ventilation. Various methods for measuring this surface pressure, defined as the average force per unit surface area acting on the visceral pleura, yielded vertical gradients that were considerably less than the hydrostatic value (1 cmH_2O/cm height) and approximately consistent with the vertical gradients in regional lung volume. It was also recognized that the pleural space is a part of the extracellular fluid compartment, and in it fluid secretion and reabsorption are determined by the same hydrostatic and oncotic pressure gradients that govern fluid exchange in other organs. Attempts to measure pleural liquid pressure yielded vertical pressure gradients approaching the hydrostatic value, and these were considerably larger than the vertical gradients in pleural surface pressure. Pleural liquid pressure was more negative than pleural surface pressure. Because the pleural fluid was believed to form a continuous sheet, it was not clear how the vertical pleural liquid pressure gradient could be less than the hydrostatic value. To reconcile the measurements of pleural surface pressure with the more negative values of pleural liquid pressure, additional forces were hypothesized. These additional forces were believed to be produced by points of contact between the parietal and visceral pleurae, either from microvilli lining the pleural surfaces or from cells in the pleural liquid (1, 2). Neither has ever been demonstrated anatomically (13). It has also been suggested that the lung may push on the chest wall at points via a load-carrying film of pleural liquid, similar in effect to that which occurs in hydrodynamic lubrication (1, 2). Such a

mechanism seems unlikely, because differences between surface and liquid pressures were also measured during apnea, when relative motion of the pleural surfaces that would generate the forces associated with hydrodynamic lubrication is absent.

In this communication we review the data supporting another formulation that reconciles this apparent paradox and points out areas where crucial confirmatory data are lacking. The major tenets of this formulation are as follows. Pleural surface pressure equals pleural liquid pressure. Pleural pressure distribution is determined by the force-balance relationship required for the lung and thoracic cavity shapes to conform to each other. Gravity influences this relationship by its action on the lung and on the configuration of the thoracic cavity, which includes the rib cage, diaphragm, abdomen, heart, and other mediastinal contents. The difference between the pleural pressure distribution dictated by the lung volume distribution and a hydrostatic gradient causes a local flow of pleural liquid with viscous pressure losses that match the difference.

Regional Lung Volume and Pleural Surface Pressure

Bronchospirometry studies in humans in the lateral decubitus position demonstrated that the dependent lung has a smaller end-expiratory volume, a larger inspired volume, and consequently a much larger ventilation per unit lung volume than the nondependent lung (58). This behavior in regional volume expansion and ventilation was matched by a larger oxygen uptake when the lungs were equilibrated with 100% oxygen, indicating that the dependent lung also has a larger perfusion. With the advent of radioactive gas techniques, it was demonstrated that vertical gradients in regional lung volume, ventilation, and perfusion are also present in the upright position (45, 65). Furthermore the vertical gradient in volume was approximately consistent with the vertical gradient of pleural pressure estimated by esophageal pressure by assuming that the overall lung pressure-volume curve could be used to predict regional volume (65). Vertical gradients in regional volume and ventilation were also demonstrated in supine humans (45).

The radioactive xenon technique, although very attractive because of its applicability to humans, has limited temporal and spatial resolution and therefore is difficult to employ in dogs and smaller animals. Whole dogs frozen in the head-up (32) and supine (39) postures revealed a vertical gradient in regional alveolar size, but with this technique there is concern about the effects of freezing on tissue properties and chest configuration. Many studies in experimental animals have inferred a vertical gradient in lung volume from measurements of pleural surface pressure. Most of this work was performed by Agostoni and associates and is summarized in excellent reviews (1, 2).

The techniques for measuring pleural pressure are discussed below. These studies demonstrated vertical differences in pleural pressure in the head-up (17, 24, 26, 37, 43, 83, 89), supine (2, 26, 36, 38, 74, 79, 89, 92), and lateral decubitus positions in experimental animals (2, 4, 26). The measured gradient was often greater than the hydrostatic gradient for a fluid with the density of the lung. Under a gravitational load, a fluid at rest produces a vertical pressure gradient equal to ρg, the product of its density ρ and the gravitational acceleration g, whereas a deformable solid in a container of the same size and shape has a vertical pressure gradient acting on its side that is less than ρg (77). Thus a vertical gradient in transpulmonary pressure greater than lung density indicates that forces in addition to gravity must be acting on the lung. This was confirmed by studies in recumbent animals showing that the weight of the abdominal contents had an important influence on the vertical gradient in costal pleural pressure (1, 2).

These studies were, in general, consistent with studies of regional volume distribution from which the pleural surface pressure distribution was inferred. Bronchospirometric studies of humans in the lateral decubitis position showed that ventilation was diverted to the nondependent lung during mechanical ventilation compared with spontaneous ventilation (75). Similar differences in ventilation distribution between spontaneously breathing and anesthetized paralyzed mechanically ventilated recumbent humans were demonstrated by the radioactive xenon technique (76). Voluntary contraction of the diaphragm in lateral decubitis humans altered the distribution of volume between dependent and nondependent lung (78). Video roentgenographic imaging of regional lung volume distribution in experimental animals with intraparenchymal lung markers demonstrated vertical and cephalocaudal gradients of lung volume in the supine position and differences in ventilation distribution between spontaneous and mechanical ventilation (42).

Measurements of regional lung density by computerized tomography in dogs (36, 38), sloths (38), and humans (15) also demonstrated vertical gradients of volume in the supine position. These observations were generally consistent with previous measurements of pleural surface pressure. These imaging techniques show that lung volume is more uniform in the prone position.

The effect of cavity shape caused partly by the weight of the heart has been shown to contribute to the vertical gradient in transpulmonary pressure in supine (59) and head-up (43) body positions in dogs. In the supine position the heart rests on the lung and moves downward with decreasing lung volume, thereby expanding the upper regions and compressing the lower regions. These regional differences may be accentuated by a cephalocaudal extension of the lung (59). In the prone position, the heart rests on the sternum so that its weight has a relatively minor effect on regional lung expansion. In the head-up dog, changing heart density by replacing the blood with mercury increased the vertical gradient in esophageal pressure (43), and these results agreed with a finite element analysis in which the weight of the heart and lung was supported by a pressure distribution over the pleural surface (18). The measured and computed vertical gradients in transpulmonary pressure were greater than ρg, the value expected from a fluidlike lung. However, when the heart weight was extrapolated to zero the predicted transpulmonary pressure gradient was slightly less than ρg. Also when the heart region was assigned a density equal to that of the lung, the finite ele-

ment model also predicted a transpulmonary pressure gradient less than ρg. The results of this simulation agreed closely with the pioneering work of West and Matthews (86).

The vertical gradient in pleural pressure did not vary systematically when lung density was reduced by increasing lung volume. In the past, studies using the counterpressure technique indicated a reduced pleural pressure gradient with passive chest expansion, although with active expansion the gradient was unchanged (1, 2, 7). In head-up dogs in which flat balloons were used to measure pleural pressure, the vertical pleural pressure gradient remained constant with chest inflation (41). More recently, in head-up dogs in which esophageal pressure measurements of pleural pressure were used, the vertical gradient in pleural pressure increased with lung inflation (43). A similar result has recently been found in the supine rabbit (93). A finite element analysis of the effect of gravity acting on the lung and heart in an upright lung showed the vertical transpulmonary pressure gradient to increase with lung inflation (18). It is important to make a distinction between the vertical gradient in alveolar size and the vertical gradient in transpulmonary pressure. The former disappears with lung inflation, because lung compliance becomes progressively smaller at higher transpulmonary pressures, even in the presence of substantial regional variations in transpulmonary pressure. Because the vertical gradient in alveolar size becomes smaller with lung inflation, mechanical ventilation with positive end-expiratory pressure results in a more uniform ventilation. This is particularly advantageous in the supine position with a large vertical gradient in transpulmonary pressure at functional residual capacity (FRC).

A more detailed review of regional lung volume and ventilation distribution is beyond the scope of this article. For the purpose of this review, the important conclusion is that regional lung volume distribution is determined by the interaction of lung and thoracic cavity shapes, with both structures being influenced by gravity (1, 2, 76, 78). The effect of the heart and other mediastinal contents and the abdomen-diaphragm is important in the upright and recumbent body positions. In all recumbent mammals studied to date, in the supine position there is a relatively steep vertical gradient of regional lung volume produced by the combined effects of gravity on the lung and a shape factor produced partly by the support of the heart (38, 42, 59). In the prone position, the regional lung volume along the vertical axis is virtually uniform, because the effect of cavity shape, including the position of the heart, offsets the effect of gravity on the lung.

Pleural pressure couples the lung to the thoracic cavity. The thin pleural liquid film with low protein concentration and low viscosity lubricates the pleural surfaces and produces a small viscous drag as the visceral and parietal costal pleural surfaces slide in opposite directions during ventilation. An excess gravity force that is not opposed by the vertical pleural pressure gradient results in a small downward flow of pleural liquid. However, the distribution of pleural surface pressure is uniquely determined by the force balance required for the lung and thoracic cavity shape to conform under any given gravitational load and activation of the respiratory muscles.

TABLE 1. *Vertical gradient in pleural pressure in head-up dogs*

Method	Gradient, cmH_2O/cm	Ref.
Pleural balloon	0.20–0.30	41, 49, 63
Counterpressure device	0.40	4
Esophageal balloon	0.40–0.42	43, 84
Alveolar size	0.50	25, 32
Rib capsule	0.53	89
Pleural catheter	0.72	17, 24
Pleural needle	0.93	83

If pleural surface pressure were uniquely determined by the matching of the lung to the chest wall according to the laws of solid body mechanics, how can the pleural liquid simultaneously follow the laws of fluid mechanics? The traditional approach to the problem as mentioned above is to consider pleural surface pressure to be different from pleural liquid pressure because of points of contact (1, 2). Although this theory has not been disproven, it is not necessary to have points of contact to reconcile liquid and surface pressures. No such points of contact have been demonstrated (13). Before we discuss viscous flow theory as it applies to the mechanics of the pleural space, it is helpful to review various techniques for measuring pleural pressure, because differences between pleural surface and liquid pressures might be attributed to the invasiveness of the measuring devices.

Measurement of Pleural Pressure

Because the pleural space is only 5–30 μm thick (8, 13, 54), it is difficult to make a reliable noninvasive direct measurement of pleural pressure. A variety of methods for measuring pleural pressure have been used. Table 1 illustrates the inconsistency of the results. It summarizes the vertical pleural pressure gradients measured in the head-up dog at FRC over the past 25 years by a variety of methods. In Table 1, pleural surface pressure was measured in the first eight studies listed and pleural liquid pressure was measured in the other studies. The values of the gradient range from 0.2 to 0.9 cmH_2O/cm. The smaller values (0.2–0.3 cmH_2O/cm) were obtained with flat pleural balloons (41, 49, 63), the larger values (0.7–0.9 cmH_2O/cm) with liquid-filled pleural catheters and needles (17, 24, 83). Intermediate values (0.4–0.5 cmH_2O/cm) for the pleural pressure gradient were determined by other methods, such as esophageal balloons (43, 84), counterpressure devices (4), alveolar size measurements (25, 32), and rib capsules (89). Because there is no universally accepted method for measuring pleural pressure directly, we are limited to pointing out some strengths and deficiencies of several methods.

Intrapleural liquid-filled catheters, rigid cannulas, and needles are relatively easy to implement and have been extensively used to measure pleural liquid pressure in experimental animals (2, 3, 8–10, 17, 24, 67–69, 71, 79). Because the pleural space is only several micrometers thick, introduction of a measuring device such as a cath-

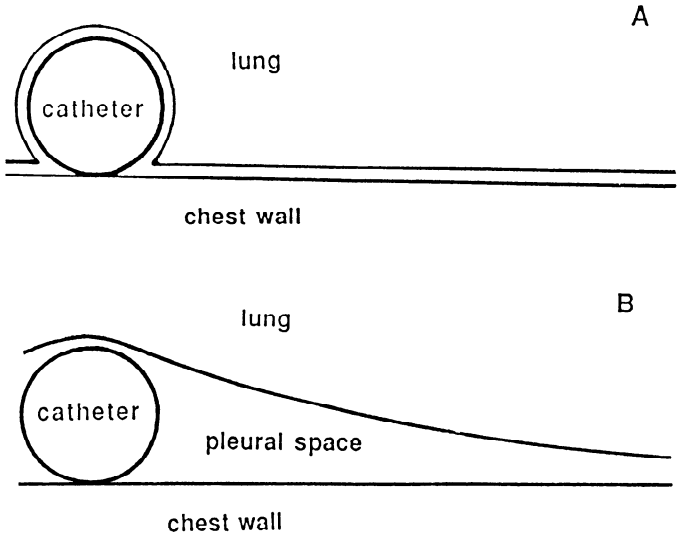

FIG. 1. Distortion around a pleural catheter. *A*: lung visceral pleura adheres closely to catheter to maintain a normal pleural space thickness. This would require a very negative pressure in the pleural space adjacent to the point where the catheter contacts the parietal pleura. *B*: distortion of the lung that occurs on flushing the catheter. Note very wide pleural space that results from relieving pressure around catheter.

eter produces a local deformation of the visceral pleura and the surrounding lung that may drastically alter the local pleural pressure (62). Even if the pressure were measured accurately, it would no longer be a reflection of the physiological state, as illustrated in Fig. 1, which shows a 1-mm-OD catheter inserted in a normally 15-μm-thick pleural space. In Fig. 1*A*, the visceral pleural surface is shown to adhere closely to the catheter and the parietal pleura to maintain a normal pleural space thickness around the catheter and the parietal pleura. A very negative pressure would be required in the area adjacent to the point of contact between the catheter and the parietal pleura to produce the large local deformation of the visceral pleura. However, such a configuration would not occur in practice, because the very negative pressure would draw fluid from adjacent regions, resulting in a pool of pleural liquid around the catheter (Fig. 1*B*). The pool of liquid that is much thicker than the normal pleural liquid space would be provided on flushing liquid through the pleural catheter. This pleural liquid would form a static column along the catheter with a vertical pressure gradient in the column equal to the hydrostatic value, similar in effect to that which occurs at relatively wide spaces adjacent to lobar margins (1–3, 9, 10, 46, 53). If the catheter were pulled up and down in the pleural space, a hydrostatic gradient would be measured. In practice, the situation is more complex, because vertical gradients in pleural liquid pressure measured by pleural catheters were less than the hydrostatic value, varying between 0.6 and 0.9 cmH_2O/cm (17, 24, 79). The slow falloff in the distortion of the pleural space from a pleural catheter (or cannula) also suggests a virtual equilibrium between the pressure at the tip of the catheter and the hydrostatic pressure gradient at a lobar margin, even though the catheter is situated several centimeters from the lobar margin (see below).

Intrapleural wick catheters have been used in an attempt to reduce the distortion of the pleural space, but like intrapleural catheters they also spread apart the pleural space and often produce results similar to those measured by intrapleural catheters (37). The argument (67) that the pressure measured by pleural cannulas eventually attains an equilibrium with the pleural pressure at undisturbed sites does not consider the deformation caused by the cannula and the mechanics of flow in the liquid that fills the deformed pleural space. A number of techniques have been developed to circumvent the problems associated with pleural catheters. All have advantages and disadvantages.

Flat air-filled pleural balloons (41) have been used to measure the average recoil of the underlying lung region adjacent to the surface of the balloon. It is assumed that the lung acts like a membrane and that the balloon-membrane interface is flat so that lung recoil is unaffected by the imposition of the pleural balloon. However, a flat pleural balloon causes some indentation of the lung surface, and the ensuing reduced recoil of the lung adjacent to the balloon, estimated using the principles of solid mechanics, would result in a reduced vertical gradient in pleural pressure (35, 89). The chest must be opened for installation of pleural balloons. On closing the chest, any residual air would accumulate in the nondependent regions of the pleural space and compress nondependent lung regions. For the above reasons, the vertical gradients in pleural pressure measured by flat pleural balloons are relatively small (0.1–0.3 cmH_2O/cm).

In the counterpressure method for measuring pleural surface pressure, a negative pressure is applied to a parietal pleural window to make it flat (1, 2, 7, 26). This method assumes that the lung surface is normally flat. Thus the magnitude of the counterpressure might be greater or less than that required to produce a normally curved pleural surface. Pleural pressure can be estimated by comparing alveolar size measured in vivo with the pressure-volume behavior measured in the isolated lung (25). The measurement of alveolar size through parietal pleural windows (25, 92, 93) also requires the removal of intercostal muscle, and therefore the lung region beneath the window would have a reduced elastic recoil. Despite these limitations, these techniques for measuring pleural pressure produced results that were, in general, consistent with measurements of lung volume distribution. However, exact comparisons are not possible, because pleural pressure and lung volume distribution have not been measured simultaneously in situ.

Two methods, the micropuncture (53, 67) and rib capsule techniques (74, 89, 92, 93), have recently been used to measure pleural pressure without distortion of the pleural space. The micropuncture technique measures pleural liquid pressure through a micropipette tip (2–5 μm diam) that is smaller than the pleural space thickness. As with the techniques that measure a counterpressure and alveolar size through pleural windows, the micropuncture technique requires the removal of intercostal muscle to puncture the parietal pleura, which would reduce the lung recoil locally. Another objection to the use of the micropuncture technique for measuring pleural liquid pressure is the uncertainty as to the exact

location of the pipette tip (67). Furthermore, with the micropuncture technique, pleural pressure can be measured only during apnea, because the glass micropipette is easily broken during ventilation. Micropuncture measurements in rabbits showed a greater vertical gradient in pleural liquid pressure in the supine position than in the prone position (53), a behavior consistent with pleural liquid pressure measured by rib capsules and with pleural surface pressure estimated by alveolar size measurements (92). These micropuncture measurements have been questioned because of results showing that pleural liquid pressure measured by micropuncture was similar to those measured by pleural cannulas and was consistent with a hydrostatic gradient (67). The differences between these micropuncture studies remain to be resolved.

In the rib capsule technique, a capsule is implanted in a rib and a small hole is made in the parietal pleura to allow pressure communication between the liquid in the capsule and the pleural liquid (74, 89, 92, 93). The rib capsule is similar in concept to the intercostal capsule (6), but the rib capsule technique avoids the removal of intercostal muscle. A limitation of the rib capsule technique is that measurements are confined to the pleural space under the ribs. When pleural pressure is subatmospheric, pleural pressure at intercostal sites might be slightly greater than that under the ribs, because the elastic recoil of the intercostal tissue layer is less than that of the rib (40). Although the rib capsule technique has limitations, it seems to be the least invasive. The vertical pleural pressure gradient measured by the rib capsule technique in dogs (89), ponies (74), and rabbits (92, 93) was greater in the supine than in the prone position, a behavior consistent with measurements of lung volume distribution (36, 38, 42, 92, 93). This is evidence for the identity between pleural surface and liquid pressures. Also these results show that, in general, pleural liquid is not in hydrostatic equilibrium. This is in contrast to previous results measured with intercostal capsules that indicated a hydrostatic gradient in pleural liquid pressure (6).

Viscous Flow of Pleural Liquid: Absence of Hydrostatic Equilibrium

Viscous flow occurs in many parts of the body. Flow though the microcirculation, microvascular filtration, clearance of fluid through interstitial beds, and flow through lymphatic vessels are examples of viscous flow. In these systems the resistance to bulk flow is primarily determined by fluid viscosity; pressure losses due to convective acceleration are negligible. Although the theory of viscous flow is a well-established branch of fluid mechanics (19), we give some simple examples of viscous flow to illustrate the concepts that are relevant to the pleural space.

First, consider steady laminar flow in a rigid uniform tube connected to a reservoir of water. Water flows out of the tube if the open end of the tube is below the level of the reservoir. The relationship between pressure P and flow $\dot{Q}$ is given by

$$P_1 - P_2 + \rho g H = 128\, \nu l \dot{Q}/(\pi d^4) \qquad (1)$$

Here P_1 is the pressure acting on the surface of the water in the reservoir, P_2 is the pressure at the outlet of the tube, ρ is water density, g is gravitational acceleration, H is vertical distance between the surface of the water in the reservoir and the tube outlet, l is tube length, d is tube diameter, and ν is fluid viscosity. The terms on the left-hand side of *Eq. 1* represent the net pressure driving flow. It consists of the pressure difference between the surface of the water in the reservoir and the outlet of the tube ($P_1 - P_2$) and the hydrostatic head $\rho g H$ due to the force of gravity acting on the water. The term on the right-hand side of *Eq. 1* is the viscous pressure loss in the tube due to flow (Poiseuille's law).

In the event that the end of the tube were to be closed, the flow would be zero and the viscous losses would be zero. *Equation 1* reduces to $P_2 - P_1 = \rho g H$, the familiar Pascal's law for a liquid at rest, which states that the pressure in a column of water at rest increases by 1 cmH_2O/cm vertical distance down the height of the column. In many situations in the body, viscous losses due to flow are negligible compared with the driving pressure, so Pascal's law is a good description of the pressure variation with height. Flow through large blood vessels is a specific example.

Consider the case where the outlet of the tube is open. Here P_1 and P_2 are both equal to the atmospheric pressure, and the driving pressure for flow is due solely to the hydrostatic head $\rho g H$ and is equal to H cmH_2O or 1 cmH_2O/cm height. The viscous pressure loss in the tube due to flow must equal the hydrostatic head. The flow in the tube depends on H, tube diameter, tube length, and viscosity of water. If we were to double tube diameter and keep other parameters constant, the flow would increase 16-fold so as to maintain the viscous pressure losses constant at 1 cmH_2O/cm height. The viscous pressure losses in a rigid tube can change only if the driving pressure changes. This requires a change in P_1, P_2, or H.

In the pleural space the forces driving flow are the pleural pressure distribution as determined by the opposing recoils of the lung and chest wall and the force of gravity acting on the pleural liquid. The geometry of the pleural space can be approximated as the space between two flat plates, where the separation of the plates is the pleural space thickness. Consider steady unidirectional viscous flow of a liquid between two vertical parallel plates separated by thickness b. The following equation relating P to $\dot{Q}$ is well known from fluid mechanics, as discussed previously (53, 90)

$$\rho g - dP/dz = 12\, \nu \dot{Q}/(L b^3) \qquad (2)$$

Here dP/dz is the gradient in pressure in the downward z direction, ρg is gravitational force per unit height acting on the liquid, and L is lateral dimension. The left-hand side of *Eq. 2* represents the net force driving flow downward, it is balanced by the term on the right-hand side, the viscous pressure losses per unit height. When the viscous losses are negligible, *Eq. 2* reduces to $dP/dz = \rho g$, the integral form of Pascal's law for a liquid at rest.

Imagine now that the plates are replaced by the lung and chest wall, the opposing elastic recoils of which pro-

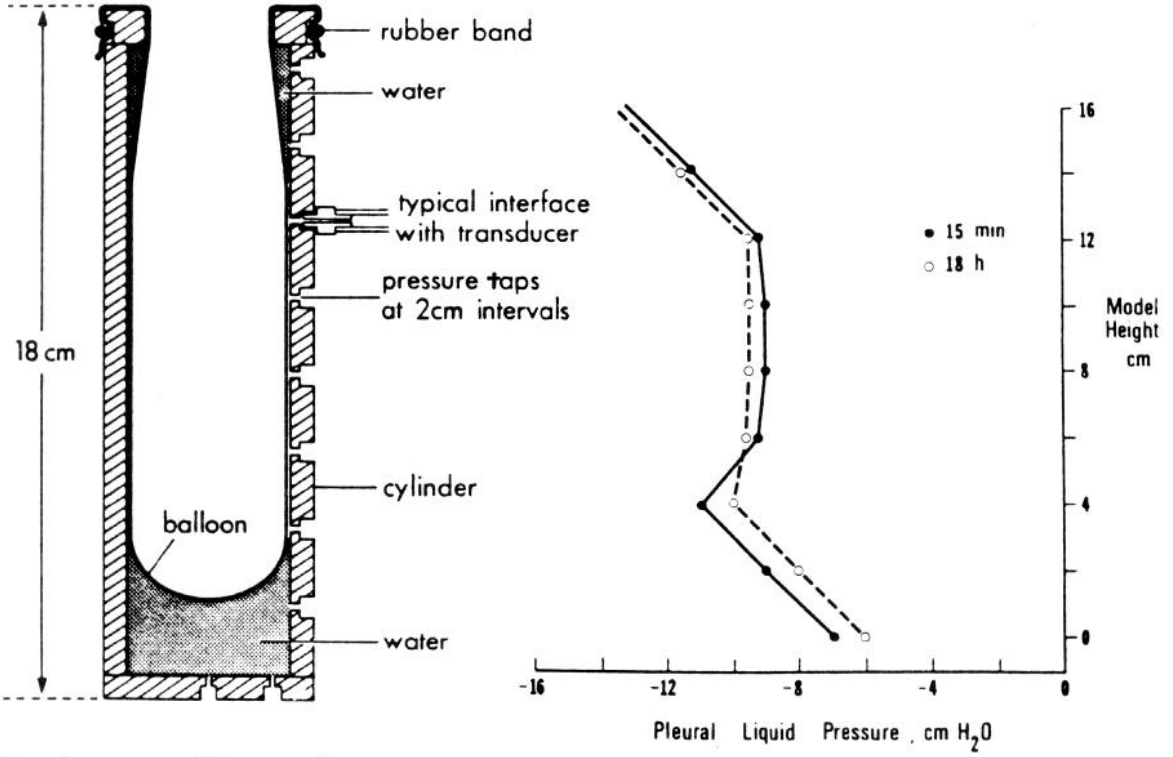

FIG. 2. Pleural pressure profile in a model of pleural space consisting of a balloon expanded within a cylinder. Pleural pressure was uniform in the middle region of the model, where the balloon adhered to the side of the cylinder, but varied by 1 cmH_2O/cm height at the 2 ends of the model, where the balloon deviated from the container. Similar values for pleural pressure were measured at 15 min and 18 h. [From Lai-Fook et al. (55).]

duce a pleural pressure gradient dP/dz. Because the volumetric compliance of the lung and chest wall is relatively large and the pleural space volume is extremely small, changes in pleural space thickness have a negligible effect on the pleural pressure. Therefore the net pressure gradient, which equals the difference between ρg and the pressure loss due to a viscous flow, is independent of the flow and thickness. For example in the prone position where the pleural pressure gradient dP/dz is zero, the viscous flow and pleural space thickness adjust so that the viscous pressure losses exactly balance the gravitational force on the liquid. These conditions were simulated in a model of the pleural space consisting of a cylindrical-shaped balloon expanded within a rigid cylindrical container (55). Pleural pressure of the model, equal to the balloon recoil, was uniform along the height of the balloon, where the balloon was expanded to a uniform diameter and the pleural space was very thin, but varied by 1 cmH_2O/cm height at the two ends of the balloon, where the space was relatively wide and the balloon recoil was nonuniform (Fig. 2). The extrapolation of these results to the pleural space has been questioned on the basis that the balloon surface was smoother than the pleural surface (5). However, viscous losses should be greater and hydrostatic equilibrium less likely for less smooth surfaces. If the pleural pressure gradient dP/dz were 0.6 cmH_2O/cm, as would occur in the supine position of many species, the net driving pressure would be $1 - 0.6 = 0.4$ cmH_2O/cm and the viscous losses would be 0.4 cmH_2O/cm.

The time course of the change in pleural space thickness that results from drainage of pleural liquid is computed to be extremely slow, as illustrated by the following idealized example in which filtration and absorption are not considered and viscous flow occurs due to the drainage of a vertical thin liquid sheet of initial uniform thickness b_0 under the force of gravity. The relationship between the thickness ratio (b/b_0) at any distance z from the top of the column and *time* t is as follows (see Ref. 19, p. 263)

$$\begin{aligned} b/b_0 &= [z/(Vt)]^{1/2} \quad z < Vt \\ &= 1 \qquad\qquad z > Vt \end{aligned} \tag{3}$$

where $V = \rho g b_0^2/(4\nu)$. This solution shows that for a vertical sheet of water of initial thickness $b_0 = 10$ μm, the thickness at 15 cm below the top of the sheet would be reduced by 60% after 1 h.

In the above examples we have discussed viscous flow in channels of uniform thickness. However, as applied to the pleural space, the presence of nonuniformities in thickness may significantly increase the flow resistance. For example, the equivalent thickness on the basis of the drainage of liquid in a balloon-in-cylinder model of the pleural space was 5 μm, whereas the mean thickness measured by gamma imaging was 20 μm (55). The measured flow was two orders of magnitude less than that predicted for a uniform channel. Similarly the relevant thickness that governs viscous flow in the pleural space may be much smaller than the average value that is measured experimentally. The presence of microvilli and cells in the pleural liquid would also serve to increase flow resistance in the pleural space.

The flow due to gravity in the pleural space is ex-

tremely small and comparable to measured pleural liquid exchange rates. For example, consider the case of a uniform pleural pressure so that $dP/dz = 0$. For a 3-kg rabbit, typical values are as follows: $L = 8$ cm, $b = 10$ μm, $\nu = 0.7 \times 10^{-2}$ dyn · s · cm^{-2}, $g = 981$ cm/s^2, $\rho = 1$ g/cm^3. Substitution of these values in *Eq. 2* results in a flow of 0.34 ml/h. This would be an upper limit, because thickness was assumed to be perfectly uniform everywhere, an unlikely situation. In any case, the estimated flow is within an order of magnitude of the pleural liquid exchange rates measured in several species (66, 69, 73, 88).

The question of homeostasis in pleural liquid volume can also be considered within the context of viscous flow concepts (14, 53, 66, 69, 73, 88). In this view, viscous flow within the pleural space is considered part of the process of pleural liquid exchange, where liquid enters the pleural space by a process of filtration across pleural capillaries with a systemic circulation, flows through the pleural space, and leaves via lymphatic stomata. In some species including humans, the visceral pleural capillaries have a systemic (i.e., bronchial) circulation (61). In sheep, pleural liquid absorption occurs entirely by stomata in the parietal pleura (14). For a steady state, the viscous flow of liquid within the pleural space must match the input flow and output flow. The average viscous flow is the sum of flow due to gravity and pleural pressure differences and motion due to ventilation and cardiogenic oscillations. Viscous flow is related to thickness through the viscous pressure losses that balance the net driving pressure. An increased filtration brought about by an increase in capillary pressure, for example, would result in a new equilibrium value for pleural liquid volume. This is achieved by an adjustment of the pleural space thickness to the filtration rate to balance the constant viscous losses. In the example represented by *Eq. 2*, the pressure loss due to viscous flow is proportional to $\dot{Q}/b^3$, so that large increases in flow can be compensated for by relatively small increases in thickness. For example, an eightfold increase in flow would be accommodated by doubling the pleural space thickness. This concept of homeostasis of pleural liquid volume on the basis of flow contrasts to that based on hydrostatics (1, 2). In the latter view, pleural fluid is absorbed by visceral pleural capillaries until there is contact between the two pleural membranes, at which point pleural liquid pressure attains a hydrostatic equilibrium. At equilibrium the pleural liquid volume determined by contact between the two pleural membranes is minimal.

Unresolved issues: effect of a hydrostatic gradient in pleural pressure at lobar margins. A cross section of a lobar margin in the rabbit measured using the light-microscopic-focusing technique (51, 54) is shown in Fig. 3. Note that the pleural liquid thickness adjacent to the margin of the middle lobe is much greater than that on the flat costal surface. This is largely due to the finite radius of curvature of the margin of the lobe that is determined by the membrane tension and the pressure in the pleural liquid adjacent to it. Several points concerning the mechanics of the lobar margin are unclear.

If the pleural pressure were to be determined by the interaction between the lung and the chest cavity, which is independent of pleural liquid flow and pleural space

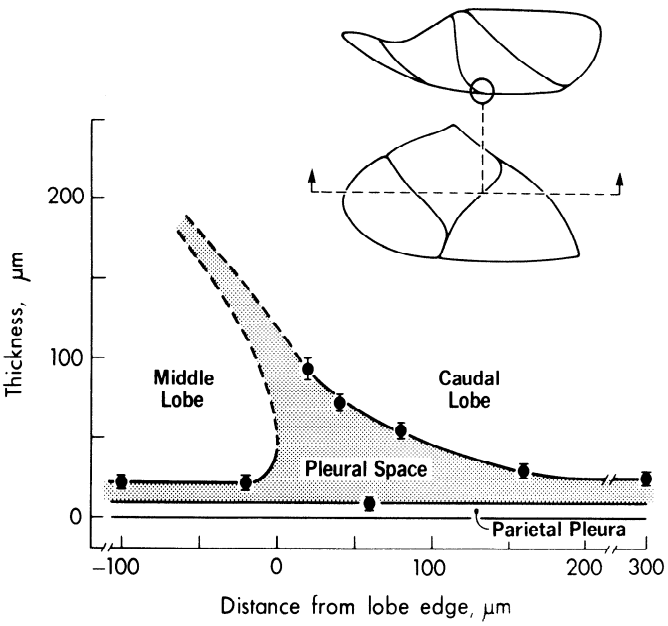

FIG. 3. Pleural space thickness profile at a lobar margin measured by light microscopy (54). Junction of a middle lobe, caudal lobe, and parietal pleura is shown. [From Lai-Fook (51).]

thickness, a hydrostatic gradient in pleural pressure should not generally be attained in the pleural space. However, there are parts of the pleural space such as at the margins of lobes where a hydrostatic gradient in pleural pressure is established (1–3, 9, 10, 46, 53). The reason for this, within the context of viscous flow concepts, is that at lobar margins the pleural space is wide enough so that the viscous losses are negligible. Also at lobar margins the vertical gradient in pleural liquid pressure must be matched by the appropriate vertical variations in lung surface curvature and pleural membrane tension (Laplace's law) that are not present on the relatively flat costal lung surface. These concepts were supported by micropuncture measurements of pleural liquid pressure in the nondependent region of prone rabbits (53) and dogs (46) that showed the pressure at the lobar margin to be more negative than on the costal surface. The flow profile required to produce the transition between the pleural pressure at the lobar margin and the greater pleural pressure on the costal surface needs to be clarified.

The presence of lobar margins may also be responsible for the relatively high vertical gradients in pleural liquid pressure measured by pleural catheters in the prone position (79), where noninvasive techniques show only a small vertical gradient (74, 89, 92, 93). In experimental animals with numerous interlobar fissures, such as the dog and rabbit, it is difficult to prevent the distortional effects of pleural catheters and cannulas from extending to lobar margins. Figure 1*B* shows the distortion of the pleural space that would be produced by a pleural catheter. The falloff in lung distortion from a catheter indenting the lung surface is proportional to $1/R$, where R is the distance from the catheter tip (35). For example, at 2 cm from a 1-mm-diam catheter, the lung distortion would be ~50 μm, much greater than the thickness of the normal pleural space and similar to the pleural liquid

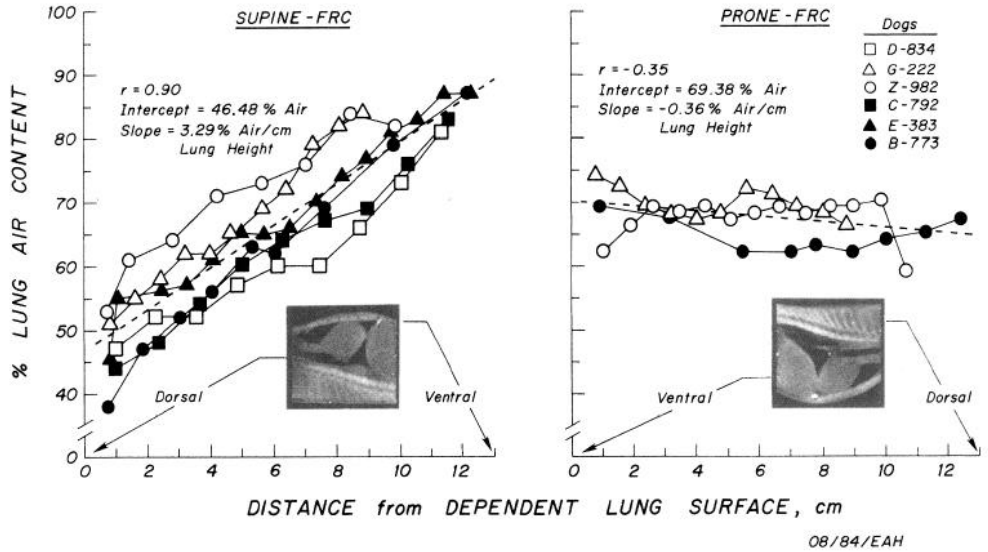

FIG. 4. Dynamic Spatial Reconstructor images of variation of lung density with height measured in supine and prone pentobarbital-anesthetized dogs (8–14.5 kg) at functional residual capacity (FRC). [Adapted from Hoffman (36).]

thickness at lobar margins (Fig. 3). The pleural pressure at the catheter tip would be nearly equal to the pressure at the lobar margin, because the intervening pleural space is relatively wide and viscous losses are relatively small. This may explain why vertical gradients in pleural liquid pressure that are close to the hydrostatic value are always measured by pleural catheters (17, 24, 79) and pleural cannulas (2, 3, 8–10, 67–69, 71).

Uniformity in pleural space thickness. The thickness of the pleural space is fairly uniform with respect to height (8, 13, 54), although a small vertical gradient in thickness has been measured (13). The reasons for this are speculative. One explanation is based on concepts involving pleural contact (1, 2); another is based on concepts involving viscous flow. In the context of viscous flow concepts, for a constant vertical pleural pressure gradient and a uniform pleural thickness, there should be a net downward flow of pleural liquid throughout the pleural space. This must occur in the presence of an expected greater filtration in dependent regions of the pleural space that arises from the increase in the vascular-to-pleural pressure difference with distance down the lung, because the hydrostatic gradient in vascular pressure is greater than the vertical gradient in pleural pressure. The uneven distribution of lymphatic stomata in the parietal pleura (14) also suggests regional differences in pleural liquid absorption. Accordingly, there should be a vertical gradient of flow in the pleural space and thus a vertical gradient in pleural space thickness. One reason why this may not occur is that ventilatory and cardiogenic motion produce flow in all directions to eliminate the regional differences in flow that result from regional differences in filtration and absorption of pleural liquid, thus providing an effective lubrication system to resolve any unevenness of pleural space thickness. Thus the nonuniformities in flow due to filtration may be small relative to the net downward flow. A net downward flow of pleural liquid requires a system to redistribute excess pleural liquid from the dependent to nondependent regions. The low-resistance pathways at lobar margins might be the primary conduits for the recirculation of this excess pleural liquid, as evident from the movement of bolus injections of dye into the pleural space (70, 71). In the absence of effective interregional mixing, a consequence of greater dependent filtration would be a lower pleural protein concentration in the dependent regions of the thorax. Such behavior has been reported for pulmonary interstitial protein as measured in visceral pleural lymphatics (12). The presence of a vertical gradient in pleural protein concentration would indicate that pleural liquid is not completely mixed and that absorption of pleural liquid by lymphatics occurs on a time scale that is smaller than that of interregional mixing.

In addition to facilitating the redistribution of pleural liquid, the presence of lobar fissures might also allow extra degrees of freedom for the lung shape to conform to changes in thoracic cavity shape during ventilation, which would reduce the nonuniformity of parenchymal stresses. However, there is little evidence to suggest that animals with interlobar fissures have a more uniform lung expansion, and lung function has been shown to be relatively unimpaired with pleural adhesions (28).

Relationship Between Nonuniform Pleural and Pulmonary Interstitial Pressures

Regional differences in interstitial pressure. The source of pleural liquid is the pleural capillaries with a systemic circulation (14). The visceral pleura is fairly permeable to water and solutes (47, 48). This suggests an equilibrium between the pulmonary interstitial pressure and pleural pressure. Thus the pressure in the subpleural interstitial space should not be greatly different from pleural pressure. Anatomically the visceral pleura enclosing the lung parenchyma is continuous at the hilum with the limiting membrane that separates the air spaces from the interstitial layer surrounding blood vessels and bronchi. The pulmonary perivascular interstitium can be considered an extension of the pleural space. Thus the mechanical principles that govern force transmission in

the pulmonary perivascular interstitium are similar in many respects to those in pleural liquid. However, the pulmonary interstitium is more heterogeneous than the pleural space. It consists of at least three distinct compartments: the alveolar wall interstitium surrounding capillaries, the perivascular interstitium of extra-alveolar blood vessels and bronchi, and the alveolar liquid space (82). Regional lung expansion affects each interstitial compartment differently.

Pulmonary interstitium does not behave like a static liquid column, so the vertical gradient in interstitial pressure is not hydrostatic. Direct measurements of interstitial pressure around small vessels and in alveolar junctions of isolated perfused lungs (21) and alveolar liquid pressure (20) in isolated unperfused lungs at constant transpulmonary pressure show that interstitial pressure is uniform with respect to height. This is due to the fact that interstitial pressure is a reflection of the parenchymal and interfacial forces acting on the interstitial boundaries. Also, the resistance to flow in the interstitium is relatively high, so gravitational forces are balanced by viscous forces as a result of an interstitial flow.

Perivascular interstitial pressure surrounding large extra-alveolar vessels is determined by the nonuniform mechanical stress in the surrounding lung parenchyma and the recoil of the vessel wall (50, 64, 80). Interstitial pressure is a direct reflection of the forces acting on the interstitial boundary. An analogous behavior occurs in the pleural space where pleural liquid pressure is determined by the opposing elastic recoils of the lung and chest wall. Perivascular pressure is slightly below the pleural pressure at FRC and falls below the pleural pressure as transpulmonary pressure increases with lung inflation (50, 80). In isolated lungs, perivascular pressure near the hilum relative to alveolar pressure decreases by 1.5 cmH_2O/cmH_2O increase in transpulmonary pressure (33, 44). In the upright chest where the vertical gradient in transpulmonary pressure ranges from 0.3 cmH_2O/cm in humans (65) to 0.5 cmH_2O/cm in the dog (89), the vertical gradient in perivascular pressure would range from 0.45 to 0.75 cmH_2O/cm. Therefore, in the intact chest the vertical gradient in perivascular pressure would be larger than the vertical gradient in transpulmonary pressure.

In the lung periphery, interstitial pressure surrounding venules (30) and in alveolar liquid (20, 30) remains nearly constant relative to pleural pressure as the lung is inflated. Therefore in the intact chest at FRC the vertical gradient in perivenular pressure and in alveolar liquid pressure would be equal to the vertical gradient in transpulmonary pressure. Interstitial pressure in the flat part of the alveolar wall has not been measured. In the absence of compressive tissue forces (34), alveolar wall interstitial pressure at FRC would be slightly below alveolar pressure (ambient pressure) because alveolar surface tension and alveolar surface curvature are relatively small. Thus alveolar wall interstitial pressure relative to alveolar pressure would be fairly uniform throughout the height of the lung whatever the vertical gradient in transpulmonary pressure may be.

Vertical gradients in interstitial pressure due to gravity-dependent gradients in lung expansion coexist with longitudinal gradients in interstitial pressure (21, 52, 64). Longitudinal gradients in interstitial pressure arise from the fact that interstitial pressure around venules and in alveolar liquid is above the pleural pressure, whereas the perivascular pressure near the hilum is below the pleural pressure. Moreover, during pulmonary edema formation, perivascular fluid cuffs are formed first around small vessels, the site of microvascular leaks (23). This is followed by the growth of fluid cuffs around larger vessels. Interstitial pressure increases as the cuffs grow, thus ensuring a favorable pressure gradient that drives fluid from the lung periphery toward the hilum.

There are dissimilarities between the pulmonary perivascular interstitium and the pleural space. Pulmonary interstitium is a solid-liquid mixture that has properties of a permeable material, whereas the pleural space is filled with a liquid. Thus the resistance to flow in pulmonary interstitium is much greater than that in the pleural space. The hydraulic resistance of pulmonary interstitium depends on the interstitial permeability, which is a function of complex osmotic interactions among the interstitial components (56), whereas the hydraulic resistance of the pleural space is determined by viscous flow of a liquid in a narrow channel.

Compliance of pulmonary interstitium and pleural space. For large changes in interstitial volume that occur during pulmonary edema formation, the compliance of the interstitium is determined primarily by the compliance of the surrounding lung parenchyma undergoing a nonuniform expansion (57, 81). The compliance of the stiffer vessel wall is negligible. The important elastic property that determines interstitial compliance is the shear modulus of the lung parenchyma. For large changes in pleural volume that accompany pleural effusions, the compliance of the pleural space is determined by the volumetric compliance (reciprocal of the bulk modulus) of the lung and the chest wall (1). Excess amounts of pleural liquid are not distributed uniformly throughout the pleural space but drain by gravity to the dependent regions (1, 54, 70).

Effect on lung fluid exchange. The rate of fluid filtration across the pulmonary microvasculature depends partly on the difference between vascular pressure and interstitial pressure. If the vertical gradient in interstitial pressure were less than the hydrostatic value, it would only partly offset the hydrostatic gradient in vascular pressure. This may result in a greater vascular-to-interstitial pressure difference and greater fluid filtration in the dependent lung regions. However, under normal conditions, extravascular lung water is uniform throughout the height of the lung, because the lymphatics are capable of absorbing all the microvascular filtrate (16, 31). During the initial stages of pulmonary edema formation, excess fluid expands the interstitium that surrounds extra-alveolar vessels and airways (82). At this stage, extravascular lung water is still fairly uniformly distributed throughout the height of the lung (72, 85), partly because redistribution of interstitial fluid is brought about by cardiogenic and ventilatory motion. A role for the bronchial circulation of peribronchial fluid cuffs in the resolution of edema fluid has been suggested (27). When the

perivascular interstitial sump is exhausted, the air spaces become flooded and there is drainage of alveolar liquid to the basal lung regions (20, 72). Excess extravascular lung water sufficient to cause alveolar flooding is partially cleared from the lung via the pleural space in sheep (22). The increased pleural liquid would in turn increase pleural pressure and compress dependent lung regions. The end effect is an increased airway closure due to blockage of peripheral dependent airways by liquid. Thus the improved gas exchange that results from the clearance of excess alveolar liquid into the pleural space might be offset by the nonuniform ventilation due to compression of peripheral airways by the increased pleural liquid.

The improved gas exchange observed when patients with respiratory distress syndrome (29) or dogs with oleic acid injury (11) are placed in the prone rather than in the supine position may be related to the more uniform lung expansion (Fig. 4), blood flow, and interstitial pressure in the prone position. In the supine position, transpulmonary pressure is lower in the dependent lung regions, and peripheral airways are more likely to collapse, in part because they are more narrow and in part because the mechanical support to the airways provided by the more compliant lung parenchyma is less. In regions of lower transpulmonary pressures, interstitial pressure is more positive, so alveolar flooding is reached earlier (57). Flooding of the air spaces results in increased airway liquid and closure of peripheral airways. The latter is exacerbated by any accompanying bronchoconstriction (91). Thus, during pulmonary edema formation that accompanies lung injury, flooding of the air spaces and closure of peripheral airways are primarily confined to dependent lung regions. This results in a ventilation-perfusion abnormality, reduction of the arterial oxygen tension, and increased intrapulmonary shunt, as observed experimentally in the supine position. By contrast, in the prone position the lung is uniformly expanded. Thus the tendency for airway closure by alveolar edema is much less in the prone than in the supine position, because the more expanded dependent lung regions in the prone position have a larger interstitial capacity and a larger alveolar surface area that retains excess liquid in alveoli (60). The net effect is more uniform ventilation and better gas exchange in the prone position.

Concluding Remarks

We have attempted to provide an explanation of pleural mechanics on the basis of principles of solid and fluid mechanics. Within this framework, many problems remain to be solved. One such problem is the redistribution of pleural liquid within the pleural space, specifically the role of ventilatory and cardiogenic motion in this redistribution. The deformation at lobar margins is another example of the interaction between viscous flow-induced forces and the structural forces in the lung. The specific details of homeostasis in pleural liquid volume are still to be worked out within the general framework of a dynamic equilibrium in which a steady-state flow through the pleural space is maintained. The distribution of the sites of leakage of pleural liquid and the pattern of flow within the pleural space are largely speculative.

This research was supported by National Heart, Lung, and Blood Institute Research Grants HL-40362, HL-36597, and HL-21584.

Address for reprint requests: S. J. Lai-Fook, Biomedical Engineering, Wenner-Gren Research Laboratory, University of Kentucky, Lexington, KY 40506-0070.

REFERENCES

1. AGOSTONI, E. Mechanics of the pleural space. In: *Handbook of Physiology. The Respiratory System. Mechanics of Breathing.* Bethesda, MD: Am. Physiol. Soc., 1986, sect. 3, vol. III, p. 531–560.
2. AGOSTONI, E. Mechanics of the pleural space. *Physiol. Rev.* 52: 57–128, 1972.
3. AGOSTONI, E., P. G. AGOSTONI, AND L. ZOCCHI. Pleural liquid pressure in the zone of apposition and in the lung zone. *Respir. Physiol.* 75: 357–370, 1989.
4. AGOSTONI, E., AND E. D'ANGELO. Comparative features of the transpulmonary pressure. *Respir. Physiol.* 11: 76–83, 1970.
5. AGOSTONI, E., AND E. D'ANGELO. Pleural liquid pressure (Letter to the editor). *J. Appl. Physiol.* 64: 1760, 1988.
6. AGOSTONI, E., E. D'ANGELO, AND M. V. BONANNI. Measurements of pleural liquid pressure without cannula. *J. Appl. Physiol.* 6: 258–260, 1969.
7. AGOSTONI, E., AND G. MISEROCCHI. Vertical gradient of transpulmonary pressure with active and artificial lung expansion. *J. Appl. Physiol.* 29: 705–712, 1970.
8. AGOSTONI, E., G. MISEROCCHI, AND M. V. BONANNI. Thickness and pressure of the pleural liquid in some mammals. *Respir. Physiol.* 6: 245–256, 1969.
9. AGOSTONI, E., L. ZOCCHI, AND P. G. AGOSTONI. Pleural liquid pressure at the caudal border of the lung. *Respir. Physiol.* 75: 117–128, 1989.
10. AGOSTONI, E., L. ZOCCHI, P. G. AGOSTONI, AND P. T. MACKLEM. Pleural pressure from abdominal to pulmonary rib cage: sweep of the lung border. *Respir. Physiol.* 75: 107–117, 1989.
11. ALBERT, R. K., D. LEASA, M. SANDERSON, H. T. ROBERTSON, AND M. P. HLASTALA. The prone position improves arterial oxygenation and reduces shunt in oleic-acid-induced acute lung injury. *Am. Rev. Respir. Dis.* 135: 628–633, 1987.
12. ALBERTINE, K. H., E. L. SCHULTZ, J. P. WIENER-KRONISH, AND N. C. STAUB. Regional differences in pleural lymphatic albumin concentration in sheep. *Am. J. Physiol.* 252 (*Heart Circ. Physiol.* 21): H64–H70, 1987.
13. ALBERTINE, K. H., J. P. WIENER-KRONISH, J. BASTACKY, AND N. C. STAUB. The structure of the pleural space in sheep (Abstract). *Federation Proc.* 48: 831, 1984.
14. ALBERTINE, K. H., J. P. WIENER-KRONISH, AND N. C. STAUB. The structure of the parietal pleura and its relationship to pleural liquid dynamics in sheep. *Anat. Rec.* 208: 401–409, 1984.
15. AMIS, T. C., H. A. JONES, AND J. M. B. HUGHES. Effects of posture on inter-regional distribution of pulmonary ventilation in man. *Respir. Physiol.* 56: 145–167, 1984.
16. BAILE, E. M., P. D. PARÉ, R. W. DAHLBY, AND J. C. HOGG. Regional distribution of extravascular water and hematocrit in the lung. *J. Appl. Physiol.* 46: 937–942, 1979.
17. BANCHERO, N., P. E. SCHWARTZ, A. G. TSAKIRIS, AND E. H. WOOD. Pleural and esophageal pressures in the upright body position. *J. Appl. Physiol.* 23: 228–234, 1967.
18. BAR-YISHAY, E., R. E. HYATT, AND J. R. RODARTE. Effect of heart weight on distribution of lung surface pressures in dogs. *J. Appl. Physiol.* 61: 712–717, 1986.
19. BATCHELOR, G. K. *An Introduction to Fluid Dynamics.* Cambridge, UK: Cambridge Univ. Press, 1967.
20. BECK, K. C., AND S. J. LAI-FOOK. Effect of height on alveolar liquid pressure in isolated edematous dog lung. *J. Appl. Physiol.* 54: 619–622, 1983.
21. BHATTACHARYA, J., M. A. GROPPER, AND N. C. STAUB. Interstitial fluid pressure gradient measured by micropuncture in excised dog lung. *J. Appl. Physiol.* 56: 271–277, 1984.
22. BROADDUS, V. C., J. P. WIENER-KRONISH, AND N. C. STAUB. Clearance of lung edema into the pleural space of volume-loaded anesthetized sheep. *J. Appl. Physiol.* 68: 2623–2630, 1990.

23. CONHAIM, R. L., S. J. LAI-FOOK, AND N. C. STAUB. Sequence of perivascular liquid accumulation in liquid-inflated dog lung lobes. *J. Appl. Physiol.* 60: 513–520, 1986.
24. COULAM, C. M., AND E. H. WOOD. Regional differences in pleural and esophageal pressures in head-up and head-down positions. *J. Appl. Physiol.* 31: 277–287, 1971.
25. D'ANGELO, E. Local alveolar size and transpulmonary pressure in situ and in isolated lungs. *Respir. Physiol.* 14: 251–266, 1972.
26. D'ANGELO, E., M. V. BONANNI, S. MICHELINI, AND E. AGOSTONI. Topography of the pleural surface pressure in rabbits and dogs. *Respir. Physiol.* 8: 204–229, 1970.
27. DEFFEBACH, M. E., N. B. CHARAN, S. LAKSHMINARAYAN, AND J. BUTLER. The bronchial circulation. *Am. Rev. Respir. Dis.* 135: 463–481, 1987.
28. DESCHAMPS, C., AND J. R. RODARTE. Effects of unilateral pleural symphysis on respiratory system mechanics and gas exchange in anesthetized dogs. *Am. Rev. Respir. Dis.* 137: 1385–1389, 1988.
29. DOUGLAS, W. W., K. REHDER, F. M. BEYNEN, A. D. SESSLER, AND H. M. MARSH. Improved oxygenation in patients with acute respiratory failure: the prone position. *Am. Rev. Respir. Dis.* 115: 559–566, 1977.
30. FIKE, C. D., S. J. LAI-FOOK, AND R. D. BLAND. Alveolar liquid pressures in newborn and adult rabbit lungs. *J. Appl. Physiol.* 64: 1629–1635, 1988.
31. FLICK, M. R., A. PEREL, W. KAGELER, AND N. C. STAUB. Regional extravascular lung water in normal sheep. *J. Appl. Physiol.* 46: 932–936, 1979.
32. GLAZIER, J. B., J. M. B. HUGHES, J. E. MALONEY, AND J. B. WEST. Vertical gradient of alveolar size in lungs of dogs frozen intact. *J. Appl. Physiol.* 23: 694–705, 1967.
33. GOSHY, M., S. J. LAI-FOOK, AND R. E. HYATT. Perivascular pressure measurements by wick-catheter technique in isolated dog lobes. *J. Appl. Physiol.* 46: 950–955, 1979.
34. GUYTON, A. C., J. C. PARKER, A. E. TAYLOR, T. E. JACKSON, AND D. S. MOFFAT. Dynamics of subatmospheric pressure in pulmonary interstitial fluid. In: *Lung Liquids,* edited by R. Porter and M. O'Connor. Amsterdam: Elsevier, 1976, p. 77. (Ciba Found. Symp. 38)
35. HAJJI, M. A., T. A. WILSON, AND S. J. LAI-FOOK. Improved measurements of the shear modulus and pleural membrane tension of the lung. *J. Appl. Physiol.* 47: 175–181, 1979.
36. HOFFMAN, E. A. Effect of body orientation on regional lung expansion: a computed tomographic approach. *J. Appl. Physiol.* 59: 468–480, 1985.
37. HOFFMAN, E. A., S. J. LAI-FOOK, J. H. WEI, AND E. H. WOOD. Pleural pressures by wick catheters. *J. Appl. Physiol.* 55: 1523–1529, 1983.
38. HOFFMAN, E. A., AND E. L. RITMAN. Effect of body orientation on regional lung expansion in dog and sloth. *J. Appl. Physiol.* 59: 481–491, 1985.
39. HOGG, J. C., AND S. NEPSZY. Regional lung volume and pleural pressure gradient estimated from lung density in dogs. *J. Appl. Physiol.* 27: 198–203, 1969.
40. HOGG, J. C., L. STEIN, R. MARTIN, AND P. T. MACKLEM. The interaction of the lung and chest wall in dogs. *Respir. Physiol.* 27: 207–221, 1976.
41. HOPPIN, F. G., JR., I. D. GREEN, AND J. MEAD. Distribution of pleural surface pressure in dogs. *J. Appl. Physiol.* 27: 863–873, 1969.
42. HUBMAYR, R. D., B. J. WALTERS, P. A. CHEVALIER, J. R. RODARTE, AND L. E. OLSON. Topographic distribution of regional lung volume in anesthetized dogs. *J. Appl. Physiol.* 54: 1048–1056, 1983.
43. HYATT, R. E., E. BAR-YISHAY, AND M. D. ABEL. Influence of the heart on the vertical gradient of transpulmonary pressure in dogs. *J. Appl. Physiol.* 58: 52–57, 1985.
44. INOUE, H., C. INOUE, AND J. HILDEBRANDT. Vascular and airway pressures and interstitial edema affect peribronchial fluid pressure. *J. Appl. Physiol.* 48: 177–185, 1980.
45. KANEKO, K., J. MILIC-EMILI, M. B. DOLOVICH, A. DAWSON, AND D. V. BATES. Regional distribution of ventilation and perfusion as a function of body position. *J. Appl. Physiol.* 21: 767–777, 1966.
46. KAPLOWITZ, M. R., AND S. J. LAI-FOOK. Pressure and dimensions of pleural liquid at lobar margins of dogs and rabbits (Abstract). *Federation Proc.* 44: 1027, 1985.
47. KIM, K. J., A. CRITZ, AND E. CRANDALL. Transport of water and solute across sheep visceral pleura. *Am. Rev. Respir. Dis.* 120: 882–892, 1979.
48. KINASEWITZ, G. T., L. J. GROOME, R. P. MARSHALL, AND J. N. DIANA. Permeability of the canine visceral pleura. *J. Appl. Physiol.* 55: 121–130, 1983.
49. KRUEGER, J. J., T. BAIN, AND J. L. PATTERSON. Elevation gradient of intrathoracic pressure. *J. Appl. Physiol.* 16: 465–468, 1961.
50. LAI-FOOK, S. J. A continuum mechanics analysis of pulmonary vascular interdependence in isolated dog lobes. *J. Appl. Physiol.* 46: 419–429, 1979.
51. LAI-FOOK, S. J. Mechanics of the pleural space: fundamental concepts. *Lung* 165: 249–267, 1987.
52. LAI-FOOK, S. J. Perivascular interstitial fluid pressure measured by micropipettes in isolated dog lung. *J. Appl. Physiol.* 52: 9–15, 1982.
53. LAI-FOOK, S. J., K. C. BECK, AND P. A. SOUTHORN. Pleural liquid pressure measured by micropipettes in rabbits. *J. Appl. Physiol.* 56: 1633–1639, 1984.
54. LAI-FOOK, S. J., AND M. R. KAPLOWITZ. Pleural liquid thickness in situ by light microscopy in five mammalian species. *J. Appl. Physiol.* 59: 603–610, 1985.
55. LAI-FOOK, S. J., D. C. PRICE, AND N. C. STAUB. Liquid thickness vs. vertical pressure gradient in a model of the pleural space. *J. Appl. Physiol.* 62: 1747–1754, 1987.
56. LAI-FOOK, S. J., N. L. ROCHESTER, AND L. V. BROWN. Effects of albumin, dextran, and hyaluronidase on pulmonary interstitial conductivity. *J. Appl. Physiol.* 67: 606–613, 1989.
57. LAI-FOOK, S. J., AND B. TOPOROFF. Pressure-volume behavior of perivascular interstitium measured in isolated dog lung. *J. Appl. Physiol.* 48: 939–946, 1980.
58. LILLINGTON, G. A., W. S. FOWLER, R. D. MILLER, AND H. F. HELMHOLTZ, JR. Nitrogen clearance rates of right and left lungs in different positions. *J. Clin. Invest.* 38: 2026–2034, 1959.
59. LIU, S., S. S. MARGULIES, AND T. A. WILSON. Deformation of the dog lung in the chest wall. *J. Appl. Physiol.* 68: 1979–1987, 1990.
60. MALO, J., J. ALI, AND L. D. H. WOOD. How does positive end-expiratory pressure reduce intrapulmonary shunt in canine pulmonary edema? *J. Appl. Physiol.* 57: 1002–1010, 1984.
61. MCLAUGHLIN, R. F., W. S. TYLER, AND R. O. CANADA. A study of the subgross pulmonary anatomy of various mammals. *Am. J. Anat.* 108: 149–159, 1961.
62. MCMAHON, S. M., S. PERMUTT, AND D. F. PROCTOR. A model to evaluate pleural surface pressure measuring devices. *J. Appl. Physiol.* 27: 886–891, 1969.
63. MCMAHON, S. M., D. F. PROCTOR, AND S. PERMUTT. Pleural surface pressure in dogs. *J. Appl. Physiol.* 27: 881–885, 1969.
64. MEAD, J., T. TAKISHIMA, AND D. LEITH. Stress distribution in lungs: a model of pulmonary elasticity. *J. Appl. Physiol.* 28: 596–608, 1970.
65. MILIC-EMILI, J., J. A. M. HENDERSON, M. B. DOLOVICH, D. TROP, AND K. KANEKO. Regional distribution of inspired gas in the lung. *J. Appl. Physiol.* 21: 749–759, 1966.
66. MINIATI, M., J. C. PARKER, M. PISTOLESI, J. T. CARTLEDGE, D. J. MARTIN, C. GIUNTINI, AND A. E. TAYLOR. Reabsorption kinetics of albumin from the pleural space of dogs. *Am. J. Physiol.* 255 (*Heart Circ. Physiol.* 24): H375–H385, 1988.
67. MISEROCCHI, G., S. KELLY, AND D. NEGRINI. Pleural and extrapleural interstitial liquid pressure measured by cannulas and micropipettes. *J. Appl. Physiol.* 65: 555–562, 1988.
68. MISEROCCHI, G., T. NAKAMURA, E. MARIANI, AND D. NEGRINI. Pleural liquid pressure over the interlobar mediastinal and diaphragmatic surfaces of the lung. *Respir. Physiol.* 46: 61–69, 1981.
69. MISEROCCHI, G., D. NEGRINI, E. MARIANI, AND M. PASSAFARO. Reabsorption of saline- or plasma-induced hydrothorax. *J. Appl. Physiol.* 54: 1574–1578, 1983.
70. MISEROCCHI, G., D. NEGRINI, M. PISTOLESI, C. R. BELLINA, M. C. GILARDI, V. BETTINARDI, AND F. ROSSITTO. Intrapleural liquid flow down a gravity-dependent hydraulic pressure gradient. *J. Appl. Physiol.* 64: 577–584, 1988.
71. MISEROCCHI, G., M. PISTOLESI, M. MINIATI, C. R. BELLINA, D. NEGRINI, AND C. GIUNTINI. Pleural liquid pressure gradients and intrapleural distribution of injected bolus. *J. Appl. Physiol.* 56: 526–532, 1984.
72. MUIR, A. L., D. L. HALL, P. DESPAS, AND J. C. HOGG. Distribution of blood flow in the lungs in acute pulmonary edema in dogs. *J. Appl. Physiol.* 33: 763–769, 1972.
73. NEGRINI, D., M. PISTOLESI, M. MINIATI, R. BELLINA, C. GIUNTINI,

AND G. MISEROCCHI. Regional protein absorption rates from the pleural cavity in dogs. *J. Appl. Physiol.* 58: 2062–2067, 1985.
74. OLSON, L. E., AND S. J. LAI-FOOK. Pleural liquid pressure measured with rib capsules in anesthetized ponies. *J. Appl. Physiol.* 64: 102–107, 1988.
75. REHDER, K., D. J. HATCH, A. D. SESSLER, H. M. MARSH, AND W. S. FOWLER. The function of each lung of anesthetized and paralysed man during mechanical ventilation. *Anesthesiology* 37: 16–26, 1972.
76. REHDER, K., A. D. SESSLER, AND J. R. RODARTE. Regional intrapulmonary gas distribution in awake and anesthetized-paralyzed man. *J. Appl. Physiol.* 42: 391–402, 1977.
77. RODARTE, J. R., AND Y. C. FUNG. Distribution of stresses in the lung. In: *Handbook of Physiology. The Respiratory System. Mechanics of Breathing.* Bethesda, MD: Am. Physiol. Soc., 1986, sect. 3, vol. III, p. 531–560.
78. ROUSSOS, C. S., Y. FUKUCHI, P. T. MACKLEM, AND L. A. ENGEL. Influence of diaphragmatic contraction on ventilation distribution in horizontal man. *J. Appl. Physiol.* 40: 417–424, 1979.
79. RUTISHAUSER, W. J., N. BANCHERO, A. G. TSAKIRIS, A. C. EDMUNDOWICZ, AND E. H. WOOD. Pleural pressures at dorsal and ventral sites in supine and prone body positions. *J. Appl. Physiol.* 21: 1500–1510, 1966.
80. SMITH, J. C., AND W. MITZNER. Analysis of pulmonary vascular interdependence in excised dog lobes. *J. Appl. Physiol.* 48: 450–467, 1980.
81. SMITH, J. C., AND W. MITZNER. Elastic characteristics of the lung perivascular interstitial space. *J. Appl. Physiol.* 54: 1717–1725, 1983.
82. STAUB, N. C., H. NAGANO, AND M. L. PEARCE. Pulmonary edema in dogs, especially the sequence of fluid accumulation in lungs. *J. Appl. Physiol.* 22: 227–240, 1967.
83. SURPRENANT, E. L., AND S. RODBARD. A hydrostatic pressure gradient in the pleural sac. *Am. Heart J.* 66: 215–220, 1963.
84. THURLBECK, W. M., AND R. M. MARSHALL. Topography of esophageal pressure in the dog. *J. Appl. Physiol.* 34: 590–596, 1973.
85. TSANG, J. Y., E. M. BAILE, AND J. C. HOGG. Relationship between regional pulmonary edema and blood flow. *J. Appl. Physiol.* 60: 449–457, 1986.
86. WEST, J. B., AND F. L. MATTHEWS. Stresses, strain, and surface pressures in the lung caused by its weight. *J. Appl. Physiol.* 32: 332–345, 1972.
87. WIENER, C. M., W. KIRK, AND R. K. ALBERT. The prone position reverses the gravitational distribution of perfusion in dog lungs with oleic acid-induced injury. *J. Appl. Physiol.* 68: 1386–1392, 1990.
88. WIENER-KRONISH, J. P., K. H. ALBERTINE, V. LICKO, AND N. C. STAUB. Protein egress and entry rates in pleural fluid and plasma in sheep. *J. Appl. Physiol.* 56: 459–463, 1984.
89. WIENER-KRONISH, J. P., M. A. GROPPER, AND S. J. LAI-FOOK. Pleural liquid pressure in dogs measured using a rib capsule. *J. Appl. Physiol.* 59: 597–602, 1985.
90. WUNDER, C. C., J. H. REED, JR., W. M. MCCONAHEY III, L. CRONIN, AND E. H. WOOD. Nature of pleural space of dogs. *J. Appl. Physiol.* 27: 637–643, 1969.
91. YAGER, D., J. P. BUTLER, J. BASTACKY, E. ISRAEL, G. SMITH, AND J. M. DRAZEN. Amplification of airway constriction due to liquid-filling of interstices. *J. Appl. Physiol.* 66: 2873–2884, 1989.
92. YANG, Q. Y., M. R. KAPLOWITZ, AND S. J. LAI-FOOK. Regional variations in lung expansion in rabbit: prone vs. supine positions. *J. Appl. Physiol.* 67: 1371–1376, 1989.
93. YANG, Q. Y., AND S. J. LAI-FOOK. Effect of airway pressure on regional lung expansion in supine and prone rabbits (Abstract). *FASEB J.* 4: A291, 1990.